Classification: Biological Sciences (Population Biology)

Human infection patterns and heterogeneous exposure in River Blindness

João A. N. Filipe[1,a], Michel Boussinesq[2], Alfons Renz[3], Richard C. Collins[4], Sarai Vivas-Martinez[5,8], María-Eugenia Grillet[6,8], Mark P. Little,[7] and María-Gloria Basáñez[1,8]

[1] Department of Infectious Disease Epidemiology, Imperial College London, Norfolk Place, London W2 1PG, UK

[2] Institut de Recherche pour le Développement, 213, rue La Fayette, Paris cedex 10, France

[3] Universität Tübingen, Institut für Tierphysiologie, AG Parasitologie, Friedhofstrasse 73, D – 72074 Tübingen, Germany

[4] P.O. Box 715, Sonoita, AZ 85637, USA

[5] Departamento de Salud Preventiva y Social, Facultad de Medicina, Universidad Central de Venezuela, Caracas, Venezuela

[6] Laboratorio de Biología de Vectores, Instituto de Zoología Tropical, Facultad de Ciencias, Universidad Central de Venezuela, Caracas, Venezuela

[7] Department of Epidemiology and Public Health, Imperial College London, Norfolk Place, London W2 1PG, UK

[8] Centro Amazónico para Investigación y Control de Enfermedades Tropicales, Estado Amazonas, Venezuela

[a] Corresponding author. Tel: +44 (0)20 759 43229; Fax: +44 (0)20 740 23927; E-mail: j.filipe@imperial.ac.uk

Manuscript pages[1]: 23 (text), 2 (figures), 3 (tables)
Supporting Information pages: 7 (text); 1 (figure); 1 (table)
Words in abstract: 171
Characters and spaces: 34,421 (text) + 11,050 (figures, tables, equations) = 45,471

[1] Abbreviations: mf: microfilariae, microfilarial; L3: third-stage (infective) larvae; ABR: annual biting rate.

Patterns of human infection with *Onchocerca volvulus* (the cause of river blindness) in different continents and ecologies are analyzed. By contrast with some geo-helminths and schistosome parasites, whose worm burdens typically exhibit a humped pattern with host age, patterns of *O. volvulus* infection vary markedly with locality. To test the hypothesis that such differences are partly due to heterogeneity in exposure to vector bites, we develop an age- and sex-structured model for intensity of infection, with parasite regulation within humans and vectors. The model is fitted to microfilarial data from savannah villages of northern Cameroon, coffee *fincas* of central Guatemala, and forest-dwelling communities of southern Venezuela, recorded before introducing ivermectin treatment. Estimates of transmission and infection loads are compared with entomological and epidemiological field data. Host age- and sex-heterogeneous exposure largely explains locale-specific infection patterns in onchocerciasis (whereas acquired protective immunity has been invoked for other helminth infections). The basic reproductive number, R_0, ranges from 5 to 8, slightly above estimates for other helminth parasites, but well below previously presented values.

Key-words: onchocerciasis, helminth, exposure, age, sex, mathematical model

Human helminth infections are a major cause of morbidity in low income countries worldwide, with over a third of the world's population infected and some 300 million people suffering consequences of severe schistosomiasis (bilharzia), intestinal helminthiases, lymphatic filariases (causing elephantiasis) and onchocerciasis (river blindness) (1−3). Large-scale control initiatives have been put in place to address these public health problems (3−5). Yet, the population and within-host processes underlying epidemiological patterns are complex and poorly understood. Among the remaining enigmas are the precise mechanisms regulating parasite abundance and determining host age-infection patterns. Understanding these mechanisms is important for explaining parasite resilience and, most crucially, for predicting post-control dynamics.

Analyses of age-infection patterns have been used to suggest processes underlying the population dynamics of helminth infections. The patterns may or not be consistent with the (null) hypothesis of a simple immigration-death process for the development of infection in hosts (6). Under this model, which assumes constant rates of parasite acquisition and mortality, infection intensity increases monotonically with age and saturates at a value determined by the ratio of these two rates. Departures from this pattern indicate that rates of parasite acquisition and/or mortality may depend on host age (through age-specific exposure or susceptibility), or on established parasite density (due to acquired immunity), or both (7, 8). A prediction of models incorporating long-lasting protective immunity is that age-intensity profiles would peak and

subsequently decline with age (7). Also, peak infection intensities would be higher and shifted towards earlier ages as transmission increases (9). The detection of significant 'peak shifts' in schistosomiasis is consistent with the acquisition of protective immunity elicited by repeated reinfection (9).

Depending on location, profiles of *O. volvulus* infection, measured by density of skin microfilariae (mf), are reported to plateau (10), peak (11) or increase (12) with host age. While some age-dependency in exposure is assumed in epidemiological models (13−16), infection-facilitated parasite establishment has been proposed as another explanation for increasing age-intensity profiles (17). However, differences in infection between males and females can be as significant as those among age-groups (18−20). Recent analyses suggest that excess mortality and blindness rates, for given mf load, are higher in men than in women (21). Yet, most existing models consider the human population without regard for sex-specific characteristics.

In this paper, we present an age- and sex-structured model for human onchocerciasis. As in previous work (22), parasite establishment in humans is determined by exposure to infective stages. The model is fitted to cross-sectional survey data from northern Cameroon, central Guatemala, and southern Venezuela. We estimate entomological parameters (annual vector biting rate) and infection levels in humans and vectors, and compare these outputs with observations. We focus on possible heterogeneity in exposure to explain age-

infection patterns specific to each sex and geographic region, and present estimates of the basic reproductive ratio, R_0, of *O. volvulus* in each environment.

Methods

Additional description of methods is given in Supporting Information.

Study areas and parasitological data. Cross-sectional surveys of skin mf load (mf/mg of skin) were conducted, prior to introduction of mass ivermectin treatment, in 37 Sudan-savannah villages (with Mboum and Dourou ethnicity) of the Vina du Nord valley in northern Cameroon (23), Mayan populations living in 9 coffee 'fincas' of central Guatemala (24), and 21 Yanomami communities of the Venezuelan Upper Orinoco basin (12, 25, 26). The number of people (and % of total population) examined was, respectively, 5,040 (50%), 872 (76-99%), and 995 (70%). The parasitological procedures applied have already been described (24, 25, 27). Average mf prevalence in each study area was about 70%. Only villages meso- and hyperendemic (mf prevalence >20%), and individuals born or resident in each village (and aged 5-80 years) with mf load ≤550 mf/mg (in line with (28)) are included in the analyses.

Entomological data. Annual vector biting rates (*ABR*) and number of infective larvae (L3) per fly for savannah forms of *Simulium damnosum s.l.* had been recorded prior to introduction of ivermectin in the Vina valley, an area without vector control (27). Pre-intervention entomological indices (biting and infection rates) have been collated for *S. ochraceum s.l.* in the Guatemalan fincas (29), and

reported for *S. guianense s.l.* and *S. incrustatum* in meso- and hyperendemic Amazonian areas (30−32).

Observations pertaining to each region (mf prevalence and intensity, *ABR*, and mean number of L3 larvae/fly) were averaged across study villages in order to obtain country- and vector-specific data with which to contrast predictions.

Ethical clearance. Informed consent from participants (or their parents or guardians) was obtained prior to skin snip sampling in each village. Communities in the study area are currently incorporated into national onchocerciasis control programs.

Model formulation. Our intensity model describes the mean number of adult worms/person and of mf/mg of skin in an age- and sex-structured human population, and the mean number of L3/fly in the vector population. The following assumptions and notation extend prior work (22):

1) The human population has a density function that depends on age (a) and sex (s), $\rho_s(a) = \rho_s \rho(a)$, where ρ_s are sex-related weights ($\sum \rho_s = 1$) and $\rho(a)$ is an exponential distribution truncated at the maximum recorded age, a_m (Table 1); it is assumed that the per capita mortality rate μ_H is constant with age, as supported by the data.

2) The mean number of adult worms and mean density of mf/mg in a person of given age and sex are $W_s(a)$ and $M_s(a)$. The mean number of L3/fly in vectors infected by mf from a person of given age and sex, is $L_s(a)$ (assuming each bloodmeal is taken from a single host and larvae develop from surviving mf ingested during that bloodmeal).

3) The rate of human-vector contact depends on age and sex of the human host. The biting rate/fly on humans, $\beta = h/g$, is determined by the interval between two consecutive bloodmeals (g) and the fraction of meals taken on humans (h) which depends on species and location (29). For a given human, the contact rate is $m\beta\Omega_s(a)$, where m is the vector to human ratio, and

$$\begin{aligned}\Omega_s(a) &= E_s\gamma_s E_0, && a < q \\ &= E_s\gamma_s \exp(-\alpha_s[a-q]), && a \geq q\end{aligned} \qquad \textbf{[1]}$$

is an age- and sex-specific measure of exposure with population average equal to 1 [ensured by normalization factors γ_s and weights E_s such that $1 = \int \rho(a)[\Omega_s(a)/E_s]da$ and $\sum E_s\rho_s = 1$], and parameters E_0, α_s and q. Relative exposure (of males with respect to females) is defined by $Q = E_M/E_F$. After an initial increase in exposure to vectors, approximated by a step function ($E_0 < 1$), during childhood period q (13, 14), contacts can either increase, decrease, or remain constant with age, depending on whether $\alpha_s < 0, \alpha_s > 0$, or $\alpha_s = 0$.

4) There is a pre-patent period, p , defined as the time between acquisition of an infective larva from a vector and migration of offspring mf to human dermal tissues (after which further transmission is possible). The value of p is fixed at 2 years (33, 34).

5) We assume the number of flies biting a host during p , $m\beta\Omega_s(a)\,p$, is large, and therefore they constitute a representative sample of the vector population. Hence, the number of incoming parasites within a human at any given time is proportional to the mean number of L3 larvae/fly in the vector population, given by

$$L = \sum_s \int \left[\rho_s(a)\Omega_s(a)\right] L_s(a)\,da = \sum_s \rho_s L_s \,, \qquad \textbf{[2]}$$

with $L_s(a)$ defined in point 2) above, and $\rho(a)\Omega_s(a)$ the probability that a vector feeds on a human of given age and sex.

6) The dynamics of mean parasite loads per human and fly are deterministic, i.e., are determined independently of the degree of variability about mean values, and, in particular, are unaffected by overdispersion. However, the numbers of mf/mg follow a given probability distribution (see below).

Assuming that parasite and host populations are at endemic equilibrium, as tested later, the dynamics of mean loads of adult worms and mf in humans are given by the following system of integro-differential equations

$$\frac{dW_s(a)}{da} = m\beta\Omega_s(a-p)\Pi_H(L)L - \sigma_W W_s(a)$$

$$\frac{dM_s(a)}{da} = \Delta W_s(a) - \sigma_M M_s(a) \qquad \textbf{[3]}$$

with L given explicitly, in terms of human mf loads, by

$$L = \frac{\beta\Pi_V(M_V)}{\sigma_L(M_V) + \bar{\alpha} + \mu_H} \sum_s \int \rho_s(a)\Omega_s(a)^2 M_s(a)\,da \qquad \textbf{[4]}$$

where $W_s(a) = M_s(a) = 0$ for $a \le p$; $\Pi_H(L)$ is the probability of establishment of acquired L3 larvae in humans as a function of L; Δ is the per capita rate at which adult worms produce mf (assuming half the worms are female and all females are mated (22)); M_V is the average mf density in the population of vectors feeding on human blood ; $\Pi_V(M_V)$ is the probability of development of ingested mf into L3 larvae within the vector as a function of M_V; σ_W and σ_M are, respectively, per capita mortality rates of adult worms and mf; $\sigma_L(M_V)$ is the rate of loss of L3 larvae per vector as a function of M_V (including parasite-induced vector mortality); and $\bar{\alpha}$ is the average of α_s over the vector population. Regulatory constraints (nonlinearities) are present both in humans and vectors, via Π_H, Π_V and σ_L (22, 29). At endemic equilibrium an explicit solution is obtained (and used for efficient estimation) by ignoring density-dependent parasite uptake by vectors, i.e., with Π_V constant and parasite abundance within flies regulated solely through parasite-induced vector mortality. Model parameters are summarized in Table 1.

Demography of the human population. Demographic parameters for each country (μ_H, ρ_s, $s = F, M$) are estimated directly from the population sample, which represents ≥ 50% of the total population. In the surveys, human age was ascertained by questioning participants during physical examination, or estimated visually when exact age was not known. An exponential distribution of survival times adequately represents the proportion of individuals surviving at age a. Since, apart from scale factor ρ_s, there is similarity in age profiles between sexes, μ_H is estimated jointly (via least squares) for both sexes. Estimates of ρ_s and μ_H for each country are presented in Table 1

Table 1

Variability in mf counts. Mf counts in individual humans are assumed to be independent random variables following a negative binomial (NB) distribution (40), with mean $M_s(a)$ and aggregation index $k_s(a)$, which depend on an individual's country, age and sex. The NB distribution is modified to allow for more flexible, age- and sex-specific numbers of zero counts. The aggregation index, $k_s(a) = M_s(a)^2 / [\sigma_s(a)^2 - M_s(a)]$, with $\sigma_s(a)^2$ the NB variance, is an inverse measure of overdispersion. Preliminary (moment) estimates of $k_s(a)$ (based on sample mean and variance within age groups (35)) suggest aggregation does not depend strongly on host sex (Fig. 1). Hence, we model

aggregation with country-specific functions of age, $k(a)$ (logistic or lognormal), with 3 free parameters (b_0, b_1, b_2).

Figure 1

Parameter estimation. Age- and sex-specific mean mf load and overdispersion are modeled for each country as described . We estimate exposure parameters *m* (vector to human ratio), *q* (period when exposure to vector bites increases with age), E_s and α_s (of the sex- and age-specific contact function $\Omega_s(a)$), and overdispersion parameters b_0, b_1, b_2 , jointly by maximum likelihood, using individual data, with demographic parameters as described and remaining parameters as in Table 1.

Predictions. Overall and sex-specific annual biting rates/person are given by $ABR = m\beta$ and $ABR_s = m\beta E_s$. Predicted overall mean adult worm and mf loads in humans (*W* and *M*), and L3 larval load/fly in the vector population (*L*) are averages of model outputs over the human and vector populations. Mean number of palpable *O. volvulus* nodules/person is estimated assuming that worm sex ratio is 1 and each palpable nodule corresponds on average to 34 females anywhere in the host body (34). Predicted overall mf prevalence (proportion of mf carriers in the human population) combines the deterministic model for mean intensity, $M_s(a)$, with the NB model for distribution of mf counts (which determines the prevalence-mean relationship). Expressions for the basic reproductive ratio, R_0 (average number of adult female worms in the human population produced by a

mated female worm during reproductive lifetime in absence of regulation (6)), and effective reproductive ratio, R_e (its equivalent in the presence of density dependence), are derived and evaluated. The latter is used to confirm endemic equilibrium status, i.e., when on average each female worm only replaces itself ($R_e \cong 1$) (6).

Assessment. Confidence intervals (CI) for parameter estimates and predictions are evaluated using nonparametric bootstrap (36), i.e., by resampling the original number of individuals of each age and sex from the dataset with replacement. Estimated CI are based on 1 000 simulations. Goodness of fit is assessed for each country by allowing a quadratic extension of the model for mean mf load: $M_s(a) + A_s a + B_s a^2$. Parameters A_s and B_s are estimated from the data, jointly with those in $M_s(a)$, and improvements in fit are tested via likelihood ratio at 5% significance.

Results

Additional results are given in Supporting Information.

Parasitological and entomological estimates. Predicted *ABR*, overall mf prevalence, and overall parasite loads in humans and flies are presented in Table 2. Predicted confidence regions are narrowest for Cameroon (the largest dataset), and contain the observed values, with two exceptions. First, CIs for mf prevalence contain the observed value of 70% in Venezuela, but are 12−14%

below observations for Cameroon and Guatemala. We attribute this small discrepancy to inaccuracy either in the model for mean intensity or, perhaps more likely, in the NB distribution assumption. As we fit intensity data, we expect more accurate predictions for intensity than for prevalence of infection, which is, nevertheless, in the range 60−70%, very close to observations. Second, mean mf load in the Amazonian focus is underestimated by ~15% (counterbalanced by a better prediction of prevalence).

The average number of female adult worms per person is in the range 40−50, in line with nodulectomy data from Burkina Faso (savannah) and Liberia (forest) (17, 28). The mean number of palpable *O. volvulus* nodules per person is 1.42 (95% CI 1.36, 1.48) in Cameroon; 1.46 (1.31, 1.60) in Guatemala; and 1.10 (0.99, 1.22) in Venezuela. Due to overdispersion, individual hosts may carry considerably more or less nodules than indicated by these averages.

The predicted *ABR* is higher for *S. ochraceum s.l.* (Guatemala), than for Amazonian vectors *S. guianense* / *S. incrustatum* (Venezuela), or savannah vectors *S. damnosum* / *S. sirbanum* (Cameroon). L3 larval loads in the vector follow the opposite trend, whereas mf prevalence (~60-70%) and mf intensity (~40 mf/mg) are very similar in all three areas. These results agree with the fact the meso-American vector is the least competent, requiring higher densities to attain similar endemicity levels (29).

Table 2

Exposure. Model fits suggest that males are subject to a higher vector biting rate than females in the study areas of Cameroon and Guatemala. Predicted ABR_M is 45 900 (95% CI: 40 900, 50 700) whereas ABR_F is 38 300 (34 300, 42 700) in Cameroon. Corresponding predictions for Guatemala are ABR_M = 241 900 (185 200, 292 300) and ABR_F = 153 084 (108 100, 191 100). By contrast, males and females are more evenly bitten in Venezuela, with ABR_M = 64 700 (50 700, 79 500) and ABR_F = 54 300 (40 300, 69 200). The significantly high men-to-women relative exposure (Q) in Guatemala, and different magnitude and sign of age-contact exponents (α_M and α_F) in Cameroon (Table 3), suggest that exposure differences in Guatemala are consistent across host ages, whereas relative exposure in Cameroon may change with age. Parameter α_s is significantly negative for women in Cameroon and men and women in the Amazonian focus, indicating that after period q, exposure continues increasing with age. By contrast, $\alpha_s \approx 0$ for men in Cameroon and men and women in Guatemala, suggesting exposure reaches a plateau.

Table 3

Age-specific overdispersion. In all study endemic areas dispersion index $k(a)$ increases with host age until 25−30 years, when k (a) ≈ 0.5 (Fig. 1).

Figure 1

Age-infection profiles. Age-profiles of mf infection show marked differences among study areas and between sexes, consistent with the exposure results

described above (Fig. 2). In N. Cameroon, mean mf intensity in men increases rapidly with age, leveling off at ~ 60 mf/mg by age 30 years. By contrast, women experience a much slower increase in infection intensity; for age < 45, skin loads in females are consistently lower than those in males. Above 45 years, however, females surpass males as their mf load rises at increasing rate, reaching 140 mf/mg at age 75. In C. Guatemala, and in agreement with other reports (11, 19), mf burden is higher in men than in women for all ages, reaching a plateau for both sexes at ~30 years. In S. Venezuela there is less difference between mf loads in men and women, with both sexes exhibiting an increase with age similar in shape and magnitude to that of women in the Vina valley. However, beyond age 30, skin infection in men tends to be higher than in women. While mf levels can reach 150 mf/mg for women living in endemic areas of northern Cameroon and among Yanomami males, they do not exceed 100 mf/mg for either men or women in central Guatemala.

Figure 2

Reproductive ratios. Predicted R_e values are very close to 1, and confidence regions include 1 (Table 3), which lends support to the assumption of endemic equilibrium. Predicted R_0 values for *O. volvulus* range from 5 (Amazonian focus) to 8 (northern Cameroon), and confidence regions from 4 to 9. R_0 estimates for other helminth parasites are of the order of 1−4 for schistosomes

and 1−6 for soil-transmitted nematodes (6). Previous, village-specific R_0 estimates for the same area of Cameroon ranged from 1 to 50+ (13, 22).

Discussion

Profiles of *O. volvulus* infection in endemic areas vary with host age and sex and geographical setting quite unlike other directly- and indirectly-transmitted helminth parasites (possibly excepting lymphatic filarial nematodes). To our knowledge, this is the first study using a full-lifecycle transmission model for fitting and comparing data across continents. Most models focus on onchocerciasis in West Africa (13−17), some in Latin America (19), but few attempt to bring epidemiological commonalities and differences into a single and coherent mathematical framework (29). Age-specific exposure to vector bites (13−16), operation of parasite-related human mortality (13, 15), and parasite-induced immunosuppression (12, 17, 26), are among the mechanisms put forward to explain observed departures of *O. volvulus* infection patterns in relation to predictions generated by simple immigration-death models (7). No model, however, has also attempted to capture sex-related heterogeneities, despite infection and morbidity patterns in some endemic areas differing markedly between males and females (11, 18−22, 24). The relative contribution of ecological (behavioral, environmental, body size) and physiological (hormonal, immunological) factors to sex-specific patterns of infection and disease has long been debated (reviewed in (35)). Most studies however, including ours, measure

parasite load indirectly through transmission stages (e.g., mf) instead of directly through adult worms.

In this paper we have proposed a novel age- and sex-structured model for the population biology of human onchocerciasis which largely explains differences in infection patterns among epidemiological settings, host ages and sexes by assuming heterogeneous exposure (rather than heterogeneous susceptibility/parasite establishment). Our formulation of exposure to vectors, in terms of host age and host sex is flexible enough to yield infection patterns that increase, saturate, or peak with host age (respectively, the so-called types I, II, and III age-intensity curves (35)). The goodness of fit achieved with this model is very satisfactory for endemic equilibrium situations, as it: 1) predicts overall transmission and infection intensities compatible with averaged (pre-control) entomological and parasitological indices; 2) reproduces age-infection profiles; and 3) provides sensible composite measures of transmission success (R_0 and R_e).

Behavior, occupation, and clothing are some of the factors that would determine exposure in different settings. Our results are compatible with knowledge of population activities in the study endemic areas. Differences in exposure between boys (fishing, swimming) and girls (occupied in the household), and between men (spending less time outside villages as they age) and women (working in the fields and collecting water in the rivers until elderly) have been quantified in N. Cameroon, and related to subsequent infection and ocular morbidity levels (20). Interestingly, and supporting the importance of

behavioral and cultural determinants of exposure, a study conducted in the same villages and ethnic groups over 10 years earlier (18) reports patterns of mf intensity with age and sex very similar to those depicted in Fig. 2A (although these authors ascribed the differences to hormonal factors, see also (37)). In Guatemala, onchocerciasis is transmitted mainly in coffee growing, mountainous areas, with men generally more exposed to vector bites while working in such areas (11, 19, 24). Among the Yanomami, use of clothing by children and adults is minimal, traditional houses lack enclosing walls, and men and women engage in similar activities around and outside villages (26, 30). However, we cannot dismiss the possible influence of host genetics, as the study populations belong to distinct ethnic groups. In West Africa, larger excess mortality of males in relation to females, due to onchocerciasis infection has been well documented (21), and could also help explain sex differences in age-profiles of mf load in Cameroon. Possible causes for either an increase or decrease in exposure to (effective) vector bites with age may include changes in host daily activity patterns, or thickening of the skin with prolonged exposure to flies and/or mf infection (24).

We are not therefore proposing that exposure is the only determinant of observed age-profiles of infection. *O. volvulus* has been shown to reduce host immunological responsiveness to parasite-specific and other antigens (reviewed in (38)), and it has been proposed that age- and/or parasite-specific immunosuppression may be responsible for increasing parasite loads with host age (12, 17). Models have been developed which make the rate of parasite

establishment an increasing function of already established worms in order to fit adult worm nodulectomy data (8, 17, 28). However, these models exclude age-dependent exposure as a plausible hypothesis to explain observed patterns, and do not deal with sex-related heterogeneities. Possible heterogeneity either in the rate of host exposure or in parasite establishment are not mutually exclusive hypotheses, and our model can easily be modified to include parasite-, age-, and sex-dependent susceptibility (35, 37, 39). In practice, given the lack of detailed exposure data, it may be difficult to disentangle exposure effects from those of within-host factors (e.g., hormonal changes, host genetics) (39). Model fitting to data categorized by endemicity level (a surrogate for transmission intensity) may help clarify the relative contribution of exposure and susceptibility.

Changes in degree of parasite overdispersion with host age have been reported widely (35); in the case of bancroftian filariasis, overdispersion decreases with age for both males and females (39). Operation of density-dependent constraints; clumped infection events; heterogeneities in parasite acquisition; negative correlation between overdispersion and intensity of infection; and sample-size biases have been proposed, among other factors, to explain observed patterns (35, 39).

Our overall estimates for the basic reproduction ratio, R_0 (ranging from 5 to 8) locate *O. volvulus* slightly above other helminths (from 1 to 6), but well below village-specific estimates previously derived without accounting for age or sex structure (13, 22). The latter were strongly influenced by reported values

of annual biting rate (to which R_0 responds linearly), and to assumed values of the fraction of vector bloodmeals taken on humans (to which R_0 responds nonlinearly). It would be important to contrast the overall estimates with those obtained by categorizing the data by endemicity levels.

Our model assumes that age-profiles of mf infection reflect those of adult worms, since mf production is conjectured to be proportional to adult worm burden and mf mortality independent of density or host age (but see (28)). For simplicity and tractability, we have included a reduction in parasite establishment within humans with number of incoming L3 larvae (22, 29), and parasite-induced vector mortality, but not density-dependent parasite uptake by vectors (22). The various density-dependent mechanisms, by acting on different processes in the parasite's lifecycle, may influence rates of reinfection differentially following treatment (40). Hence, models aiming at predicting post-control, non-endemic dynamics, and feasibility of local elimination with current control methods, will have to test hypotheses as to which regulatory mechanisms are most influential.

Acknowledgements

We thank Tom Churcher and Paul Clarke for insightful discussions during model development, and Sébastien Pion and John Williams for helpful comments on the manuscript. JF and MGB gratefully acknowledge funding from MRC, UK.

Contributorship: JF developed the models and analyses with discussions with MGB and MPL. MB and AR collected, respectively, parasitological and entomological data in Cameroon, RCC in Guatemala, and SVM, MEG and MGB in Venezuela. JF and MGB wrote the paper and all coauthors contributed to the final manuscript.

Conflict of interest: there is no conflict of interests to report.

References

1. Anon (Editorial). (2004) *Lancet* **364,** 1993−1994.
2. Michael, E., Bundy, D. A. & Grenfell, B. T. (1996) *Parasitology* **112,** 409−428.
3. Richards, F. O. Jr., Boatin, B., Sauerbrey, M. & Sékétéli, A. (2001) *Trends Parasitol*. **17,** 558−563.
4. Molyneux, D. H. (2004) *Lancet* **364,** 380−383.
5. Fenwick, A., Savioli, L., Engels, D., Bergquist, N. R. & Todd, M. H. (2003) *Trends Parasitol*. **19,** 509−515.
6. Anderson, R. M. & May, R. M. (1991) *Infectious Diseases of Humans: Dynamics and Control* (Oxford Univ. Press, Oxford).
7. Anderson, R. M. & May, R. M. (1985) *Nature* **315,** 493−496.
8. Duerr, H. P., Dietz, K. & Eichner, M. (2003) *Parasitology* **126,** 87−101.
9. Woolhouse, M. E. J., Taylor, P., Matanhire, D. & Chandiwana, S. K. (1991) *Nature* **351,** 757−758.
10. Kirkwood, B., Smith, P., Marshall, T. & Prost, A. (1983) *Trans. R. Soc. Trop. Med. Hyg.* **77,** 857−861.
11. Tada, I., Aoki, Y., Rimola, C. E., Ikeda, T., Matsuo, F., Ochoa, J. O., Recinos, M., Sato, S., Godoy, H. A., Orellana, J. *et al.* (1979) *Am. J. Trop. Med. Hyg*. **28,** 67−71.
12. Botto, C., Gillespie, A. J., Vivas-Martínez, S., Martínez, N., Planchart, S., Basáñez, M.-G. & Bradley, J. E. (1999) *Trans. R. Soc. Trop. Med. Hyg.* **93,** 25−30.
13. Dietz, K. (1982) in *Population Dynamics of Infectious Diseases*, ed. Anderson, R. M. (Chapman & Hall, London), pp. 209−241.
14. Remme, J., Ba, O., Dadzie, K. Y. & Karam, M. (1986) *Bull. World Health Organ*. **64,** 667−681.
15. Plaisier, A. P., Van Oortmarssen, G. J., Habbema, J. D. F., Remme, J. & Alley, E. S. (1990) *Comput. Methods Programs Biomed*. **31,** 43−56.
16. Davies, J. B. (1993). *Ann. Trop. Med. Parasitol*. **87,** 41−63.

17. Duerr, H. P., Dietz, K., Schulz-Key, H., Büttner, D. W. & Eichner, M. (2003) *Trans. R. Soc. Trop. Med. Hyg.* **97,** 242−250.
18. Anderson, J., Fuglsang, H., Hamilton, P. J. S. & Marshall, T. F. De C. (1974) *Trans. R. Soc. Trop. Med. Hyg.* **68,** 209−222.
19. Wada, Y. (1982) *Jpn. J. Med. Sci. Biol.* **35,** 183−196.
20. Renz, A., Fuglsang, H. & Anderson, J. (1987) *Ann. Trop. Med. Parasitol*. **81,** 253−262.
21. Little, M. P., Breitling, L. P., Basáñez, M.-G., Alley, E. S. & Boatin, B. A. (2004) *Lancet* **363,** 1514−1521.
22. Basáñez, M.-G. & Boussinesq, M. (1999) *Philos. Trans. R. Soc. Lond. B Biol. Sci*. **354,** 809−826.
23. Boussinesq, M., Prod'hon, J. & Chippaux, J. P. (1997) *Trans. R. Soc. Trop. Med. Hyg.* **91,** 82−86.
24. Brandling Bennett, A. D., Anderson, J., Fuglsang, H. & Collins, R. (1981) *Am. J. Trop. Med. Hyg*. **30,** 970−981.
25. Basáñez, M.-G. & Yarzábal, L. (1989) in *Parasitic Diseases: Treatment and Control*, ed. Miller, M.J. & Love, E.J. (CRC Press, Florida), pp. 231−256.
26. Vivas-Martínez, S., Basáñez, M.-G, Botto, C., Rojas, S., García, M., Pacheco, M. & Curtis, C. F. (2000) *Parasitology* **121,** 513−525.
27. Renz, A. (1987). *Ann. Trop. Med. Parasitol*. **81,** 239−252.
28. Duerr, H. P., Dietz, K., Schulz-Key, H., Büttner, D. W. & Eichner, M. (2004) *Int. J. Parasitol.* **34,** 463−473.
29. Basáñez, M.-G., Collins, R. C., Porter, C. H., Little, M. P. & Brandling-Bennett, D. (2002). *Am. J. Trop. Med. Hyg.* **67,** 669−679.
30. Vivas-Martínez, S., Basáñez, M.-G., Grillet, M.-E., Weiss, H., Botto, C., García, M., Villamizar, N. J. & Chavasse, D. C. (1998) *Trans. R. Soc. Trop. Med. Hyg.* **92,** 613−620.
31. Grillet, M.-E., Basáñez, M.-G., Vivas-Martínez, S., Villamizar, N., Frontado, H., Cortez, J., Coronel, P. & Botto, C. (2001) *J. Med. Entomol*. **38,** 520−530.
32. Gowtage-Sequeira, S., Higazi, T., Unnasch, T. R & Basáñez, M.-G. (2002) *Br. Simuliid Group Bull.* **18,** 13−15.
33. Prost, A. (1980) *Bull. World Health Organ*. **58,** 923−925 [French].
34. Duke, B. O. L (1993) *Trop. Med. Parasitol.* **44,** 61−68.
35. Wilson, K., Bjørnstad, O. N., Dobson, A. P., Merler, S., Poglayen, G., Randolph, S. E., Read, A. F. & Skorping, A. (2003) in *Ecology of Wildlife Diseases*, ed. Hudson, P. J., Rizzoli, A., Grenfell, B. T., Heesterbeek, H. & Dobson, A. P. (Oxford Univ. Press, Oxford), pp. 6−44.
36. Efron, B. & Tibshirani, R. J. (1993) *An Introduction to the Bootstrap*. (Chapman & Hall/CRC Press, London).
37. Brabin, L. (1990) *Acta Leiden.* **59**, 413−426.
38. Bradley, J. E., Whitworth, J. & Basáñez, M.-G. (in press) in *Topley and Wilson's Microbiology and Microbial Infections 10th edition, Parasitology volume*, ed. Wakelin, D., Cox, F. E. G., Despommier, D. & Gillespie, S. (Edward Arnold Publishers, Ltd.)
39. Alexander, N. D. E & Grenfell, B. T. (1999) *Parasitology* **119,** 151−156.
40. Churcher, T. S., Filipe, J. A. N. & Basáñez, M.-G. Density dependence and the control of helminth parasites. *Am. Naturalist* (under review).

Figure legends

Figure 1. Observed and predicted age-profiles of the overdispersion parameter, $k(a)$: moment estimates within 3-yr age-groups (open circles: females, closed circles: males); direct fit to moment estimates (thick line); and full model fitted to individual data jointly with the model for $M_s(a)$ (thin line). Direct and full-model fits use the same 3-parameter function: logistic (Cameroon) or lognormal (Guatemala and Venezuela). The full model agrees with the moment estimates, supporting our model for overdispersion.

Figure 2. Observed and predicted age-profiles of mf load by sex and country: mean and standard error of observations within ~10-yr age-groups (open circles: females, closed circles: males), and model fitted to individual data (Cameroon: ~5000, Guatemala: ~900, and Venezuela: ~1000 individuals); solid lines (males), broken lines (females).

Table 1. Parameters of the model

Symbol	Description / equation	Values and units			Comments / Ref(s).
		Cameroon	Guatemala	Venezuela	
$k_s(a)$	Overdispersion parameter of the negative binomial for mf load with host age a and sex s	estimated (Fig. 1)			
ρ_F; ρ_M	Fraction of human females; males	0.45; 0.55	0.42; 0.58	0.40; 0.60	Sample
$\rho(a)$	Proportion of humans at age a (function of μ_H)	estimated (Fig. 3)			
μ_H	Per capita mortality rate of human host	0.040 yr^{-1}	0.040 yr^{-1}	0.032 yr^{-1}	(Fig. 3)
a_m	Maximum human age	80 yr	80 yr	70 yr	Sample
β	Biting rate per fly on humans = h/g with g = 0.0096 yr (3.5 days) for all vectors				(22)
h	Fraction of bloodmeals taken on humans	0.3	0.6*	0.5†	(22, 29)
m	Average number of vectors per human	estimated (Table 2)			—
E_s	Sex-specific exposure	estimated (Table 3)			—
E_0	Relative exposure at age 0 in relation to age q	0.10	0.10	0.05	‡
q	Period of initial increase in exposure to vector bites during childhood	estimated (Table 3)			—
α_s	Rate of change in contact rate with age in human of sex s	estimated (Table 3)			—
Q	Relative male-to-female exposure = E_M / E_F.	estimated (Table 3)			—
p	Pre-patent period from infective bite to mf migration to human skin	2 yr			(33, 34)
Δ	Per capita fecundity rate of female worms scaled per mg of skin assuming all females are mated and sex ratio is 1	0.337 yr^{-1}			(22)
σ_W, σ_M	Per capita mortality rates of adult worms, skin mf	0.1 yr^{-1}, 0.8 yr^{-1}			(34)

* Chosen to be twice the value for Cameroon (22) and within range previously explored (29).
† Chosen as to reflect maximum uncertainty.
‡ Selected to give R_e closer to 1. Parameters E_0 and q are highly correlated.

Table 2. Entomological and parasitological estimates

Country (vector)		Annual biting rate[§] (person^{-1} yr^{-1})	Mf prevalence (%)	Mf load (mf/mg)	Infective larval load[§] (L3/fly)
Cameroon	Observed	42,800	71.0	39.4	0.032
(*S. damnosum s.s.*	Estimate	42,500	61.0	38.1	0.031
/ S. *sirbanum*)	(95% CI)	(38 700, 46 400)	(60.0, 62.0)	(36.4, 39.8)	(0.029, 0.035)
Guatemala	Observed	205,700	70.0	40.3	0.005
(*S. ochraceum s.l.*)	Estimate	202,800	63.0	40.2	0.006
	(95% CI)	(154 000, 245 600)	(61.0, 65.0)	(36.3, 44.5)	(0.005, 0.007)
Venezuela	Observed	63,970	70.0	38.7	0.012
(*S. guianense s.l.*	Estimate	60,500	71.0	29.2	0.013
S. incrustatum)	(95% CI)	(47 500, 74 400)	(69.0, 73.0)	(26.1, 32.4)	(0.012, 0.014)

[§] These observations are independent from the data to which the model has been fitted.

Table 3. **Exposure and epidemiological estimates**

Country		q (yr)	α_F	α_M	$Q=E_M/E_F$	R_0	R_e
Cameroon	Estimate	0.0	-0.023	0.007	1.20	7.7	0.99
	(95% CI)	(0.0, 0.0)	(-0.030, -0.017)	(0.002, 0.012)	(1.07,1.33)	(7.0, 8.4)	(0.91, 1.04)
Guatemala	Estimate	2.6	0.004	0.007	1.61	7.3	1.02
	(95% CI)	(2.0, 4.2)	(-0.010, 0.020)	(-0.002, 0.019)	(1.31, 2.04)	(5.6, 8.9)	(0.93, 1.06)
Venezuela	Estimate	2.3	-0.023	-0.039	1.19	5.3	0.97
	(95% CI)	(1.6, 4.8)	(-0.035,-0.011)	(-0.048,-0.027)	(0.98, 1.47)	(4.1, 6.5)	(0.90, 1.03)

Figure 1

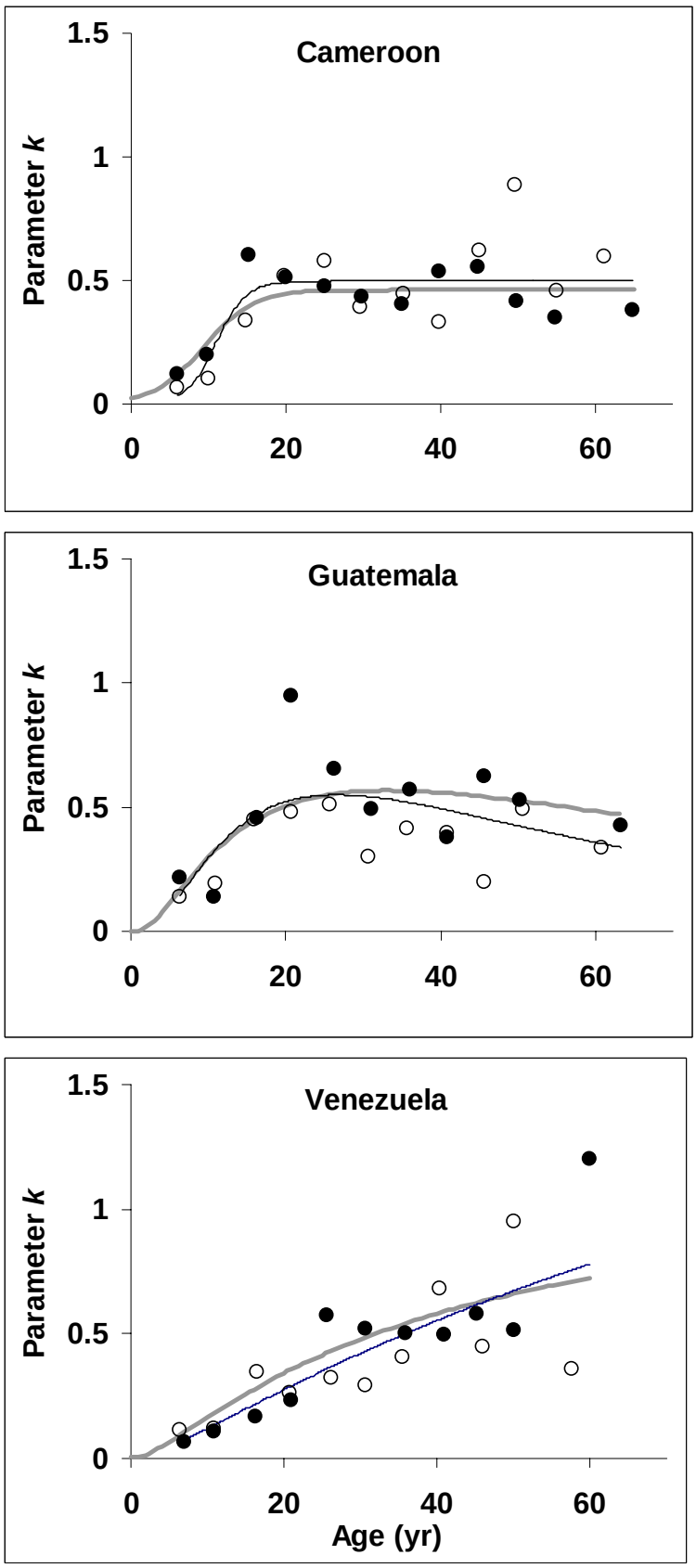
Cameroon
Guatemala
Venezuela
Parameter k
1.5
1
0.5
0
0
20
40
60
Age (yr)

Figure 2

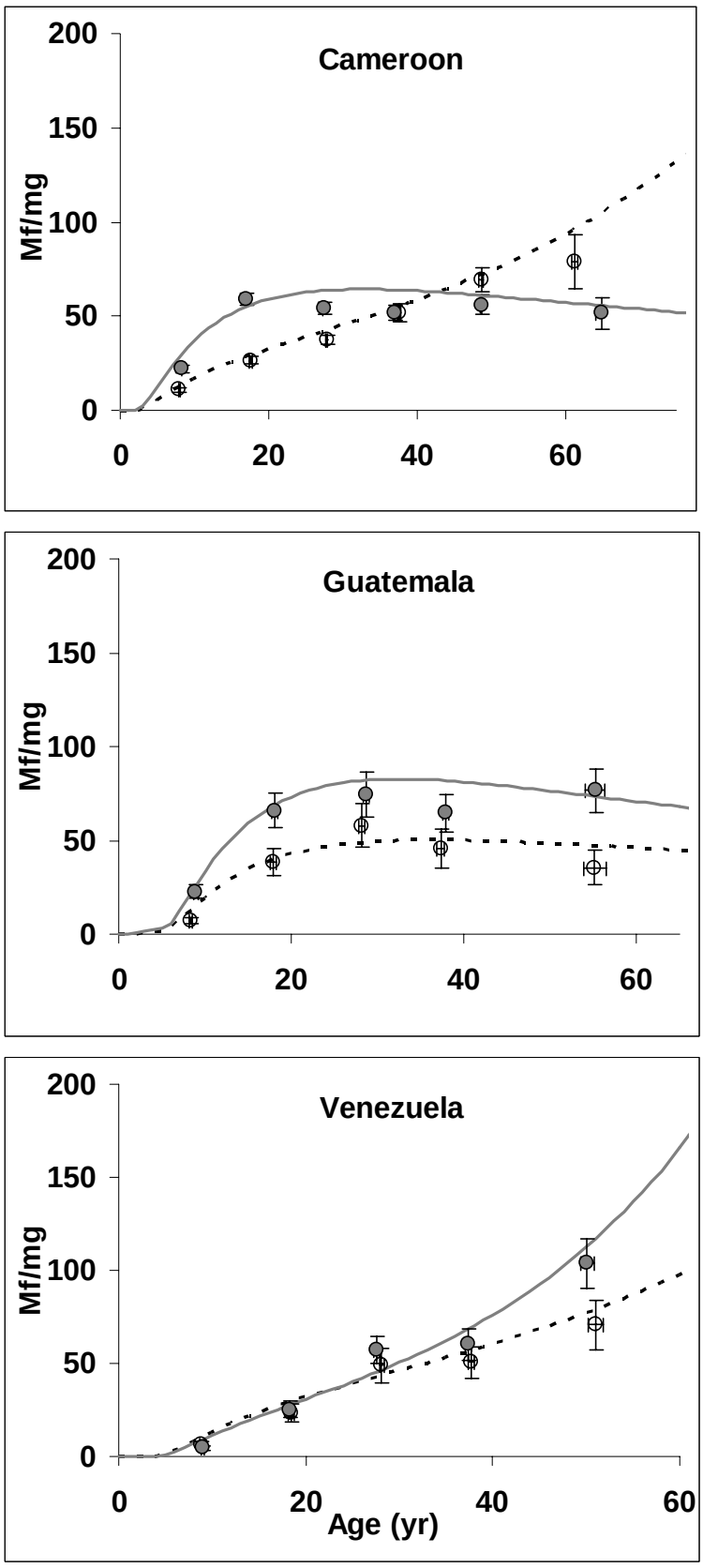
Cameroon
Guatemala
Venezuela
Mf/mg
Age (yr)
0
20
40
60
50
100
150
200

Supporting Information

Description of data sets

In all surveys, a Holth-type corneoscleral punch was used for skin-snipping (≥ 2 biopsies were taken from each patient). Snips were incubated during 8−24 h, and weighed to obtain the arithmetic mean number of mf/mg of skin. For the Cameroonian data, a mean weight of 2.84 mg per snip was assumed (41).

One of the criteria for including villages in each study (mf prevalence >20%), is based on the definition of endemicity levels adopted by the Onchocerciasis Elimination Program for the Americas (42).

Although in Guatemala there had been control interventions based on nodulectomy (24, 29), these are thought to have had negligible impact (43), so we consider that the parasite population was at equilibrium.

The age profiles of the populations studied in each country are characterized, to good approximation, by an exponential distribution of survival times (Fig. 3)

Figure 3

Derivation of the model for mean parasite loads

The dynamics of the mean loads of parasite stages in humans and vectors are described by the following system of integral partial-differential equations,

$$\begin{aligned} \frac{\partial W_s(a)}{\partial t} + \frac{\partial W_s(a)}{\partial a} &= m\beta\, \Omega_s(a-p)\, \Pi_H[L, W_s(a), a]\, L - \sigma_W\, W_s(a) \\ \frac{\partial M_s(a)}{\partial t} + \frac{\partial M_s(a)}{\partial a} &= \Delta\, W_s(a) - \sigma_M\, M_s(a) \end{aligned} \qquad [5]$$

$$\frac{\partial L_s(a)}{\partial t} + \frac{\partial L_s(a)}{\partial a} = \beta\, \Omega_s(a)\, \Pi_V[M_s(a)]\, M_s(a) - \sigma_L[M_s(a)]\, L_s(a) \qquad [6]$$

where explicit time dependency in W_s, M_s, L_s and L is omitted, and parasite loads are zero for $a < p$. We define here quantities not defined in the main text: $\Pi_H[L, W_s(a), a] = S_s(a)\, \delta_H[L, W_s(a)]\, e^{-\mu_H p}$, the probability of establishment of incoming L3 larvae, with $S_s(a)$ the host's susceptibility, $\delta_H[L, W_s(a)]$ the probability of an infective larva developing into an adult worm as a function of incoming larvae and/or established worms, and $e^{-\mu_H p}$ the host's probability of survival during p; $\Delta = \phi F / 2$, with ϕ the mating probability, F the fecundity rate of a female adult worm scaled per mg of skin (22), and 1/2 the proportion of female worms (we assume that every female is fertilized, i.e., $\phi = 1$, in a pre-control, highly overdispersed and polygamous parasite population (7, 22)); and $\sigma_L[M_s(a)] = \sigma_{L_0} + (a_H / g) + \mu_V + \alpha_V M_s(a)$, with a_H the probability that an L3 larva is shed per vector bite, σ_{L_0} and μ_V the per capita background mortality rates of L3 larvae and vectors, and α_V the rate of vector mortality induced per mf (22, 29).

There is density dependence in parasite development within humans and vectors, and in vector mortality. Note that this formulation allows for a clear distinction between age- and sex-specific exposure and susceptibility. Here, we consider that all hosts have identical susceptibility ($S_s(a) = 1$), and the probability that an L3 larva develops into an adult worm has the form (22, 29),

$$\delta_H(L) = \frac{\delta_{H_0} + \delta_{H_\infty} c_H m \beta L}{1 + c_H m \beta L}. \qquad [7]$$

with parameters described in Table 4.

In order to determine the mean infective larval load in vectors, $L(t)$, in [5], we use definition [2], extended to allow for time dependency, where $L_s(t) = \int \rho(a) \Omega_s(a) L_s(a,t)\, da$ is the mean L3 load/fly transmitted from humans of sex s. An equation for $L_s(t)$ is derived by multiplying [6] by $\rho(a)\, \Omega_s(a)$ and integrating over host age. Since the dynamics of L3 larvae in flies are much faster than those of the other parasite stages (Tables 1, 4), we assume that vector larval load is at equilibrium with respect to changes in loads of other parasite stages, giving

$$L_s(t) = \frac{\beta \int_p^{a_m} \rho(a) \Omega_s(a)^2 \delta_V[M_s(a,t)] M_s(a,t)\, da}{\sigma_L[M_{V,s}(t)] + \alpha_s + \mu_H}, \qquad [8]$$

where we set $L_s(0) = 0$, omit negligible terms (evaluated at $a = a_m$), and, for simplicity, replace $M_s(a,t)$ with $M_{V,s}(t)$ in the density-dependent vector mortality

rate, where $M_{V,s}(t) = \int \rho(a)\Omega_s(a)M_s(a,t)\,da$ is the average density of mf in the population of vectors feeding on blood from humans of given sex.

An expression for the effective reproductive ratio, R_e, defined as the average number of adult female worms produced by an adult female worm during its reproductive lifetime in the presence of density dependence, can be derived,

$$R_e(t) = \sum_s \int_p^{a_m} \rho_s(a)\frac{\Delta}{\sigma_W}\frac{m\beta\Omega_s(a)}{\sigma_M}\frac{\delta_V[M_s(a,t)]}{\sigma_L[M_s(a,t)]}da \times \sum_{s'} \int_0^{a_m-p} \rho_{s'}(a')\beta\Omega_{s'}(a')\delta_H[L(t)]e^{-\mu_H p}\,da' \qquad [9]$$

The basic reproductive ratio, R_0(t), is the density-independent version of [9].

Equations [5], [6] and [8] form a closed system of non-linear integro-differential equations. Assuming parasite and human populations are at endemic equilibrium, equations [5] and [8] become equations [3] and [4] in the main text (using $L = \sum \rho_s L_s$). In deriving the latter equations, we replace $M_{V,s}$ with M_V and α_s with $\bar{\alpha}$, and consider that the probability of larval development within the vector (43) is density-independent, $\Pi_V[M_s(a)] = \delta_{V_0}$, i.e., regulation within the vector occurs only through parasite-induced mortality (13). These simplifications allow for an explicit solution of the model, which is used to reduce numeric computation and increase efficiency of parameter estimation. Values used for parameters introduced above are given in Table 4.

Table 4

Parameter estimation

Skin snip counts of mf (x_i) in individual humans (i) in either of the study areas are assumed to follow a negative binomial (NB) distribution, with mean $M_s(a)$, aggregation index $k_s(a) = M_s(a)^2/[\sigma_s^2(a) - M_s(a)]$, and variance $\sigma_s^2(a)$, specific to the country, age and sex of the individual. The likelihood of the parameters ($\theta = \{m, q, E_s, \alpha_s, b_0, b_1, b_2\}$), given the data ($\mathbf{x} = \{x_i\}$), is

$$L(\theta \mid \mathbf{x}) = \prod_i \left[\frac{\Gamma(x_i + k_i)}{\Gamma(k_i) x_i!} p_i^{x_i} (1 - p_i)^{k_i} \right] \qquad [10]$$

where Γ is the Gamma function; the product runs over every individual i, and the index in M_i, k_i, and $p_i = \frac{M_i}{M_i + k_i}$ refers to the individual's country, age and sex.

In order to get insight, we first evaluated $k_s(a)$ empirically for groups of individuals of the same country, age and sex, using a sample-moment estimator corrected for group size (n), $\hat{k} = [\hat{M}^2 - s^2/n]/[s^2 - \hat{M}]$ (35, 44). The results (Fig. 1) suggest that $k_s(a)$ can be approximated by a 3-parameter function of age, with parameters common to both sexes. We adopt lognormal ($k(a) = b_0 \exp(-b_1[\log(a/b_2)]^2)$) or logistic ($k(a) = b_0/[1+\exp(-[a - b_1]/b_2)]$) functions, depending on country. Parameters are estimated by maximizing the log-likelihood, with M_i being the solution of [3] and [4], and k_i as described, using a simplex optimization algorithm (NAG routine E04CC). Fitting the data

with sex-specific k parameters did not yield significant improvement (results not shown).

Zero-inflated distribution: We allow for the number of zero mf counts to differ from that of the NB distribution. For an individual i, we set the probability of a zero count proportional to $(1-p_i)^{k_i\Psi}$. To ensure normalization, the original probability of each count is divided by $1+(1-p_i)^{k_i\Psi}-(1-p_i)^{k_i}$. The value $\Psi=0.7$ is used for the three countries, as it generally provides superior model fits to the data and maximum-likelihood estimates of $k(a)$ close to empirical estimates (Fig. 1). This extension of the NB relates to previous approaches (45, 46) and can be interpreted as allowing for false-negative mf counts, non-susceptible hosts (putative immune (38)), or simply a more flexible distribution.

Calculation of prevalence

Within a group of individuals of given country, age and sex, denoted j, the predicted prevalence of mf infection, P_j, is 1 minus the probability of zero counts,

$$P_j = 1-\frac{(1-p_j)^{k_j\Psi}}{1+(1-p_j)^{k_j\Psi}-(1-p_j)^{k_j}} = \frac{1-(1+M_j/k_j)^{k_j}}{1+(1+M_j/k_j)^{-k_j\Psi}-(1+M_j/k_j)^{-k_j}}\,.$$

The predicted overall prevalence of infection is the average over the human population of the age- and sex-specific prevalence,

$P=\sum\rho_s\int\rho(a)\,P_s(a)\,da$.

Goodness of fit

The goodness of model fit can be assessed qualitatively from Fig. 2. In addition, a quadratic augmentation of the model for age- and sex-specific mean mf load yields a likelihood-ratio statistic that is non-significant for either country (P = 0.18, 0.09 and 0.07 for Cameroon, Guatemala, and Venezuela, respectively). Analyses of residuals (quadratic fits) suggest the fit is best for the Cameroonian dataset (the largest) and least good for the Venezuelan dataset (smaller and collated over a longer time-span (12, 25, 26)). In addition, difficulties in estimating host age may have a greater effect in smaller studies.

References

41. Prost, A. & Prod'hon, J. (1978) *Med. Trop. Mars*. **38**, 519−532.
42. Blanks, J., Richards, F., Beltrán, F., Collins, R., Álvarez, E., Zea-Flores, G., Bauler, B., Cedillos, R., Heisler, M., Brandling-Bennett *et al.* (1998) *Pan. Am. J. Pub. Health* **3**, 367−374**.**
43. Basáñez, M.-G. & Ricárdez-Esquinca, J. (2001) *Trends Parasitol* **17,** 430−438
44. Elliott, J. M. (1977) *Some Methods for the Statistical Analysis of Samples of Benthic Invertebrates*. *Freshwater Biol. Assoc. Sci. Publ*. 25 (Titus Wilson & Son, Cumbria, UK).
45. Grenfell, B.T., Das, P.K., Rajagopalan, P.K. & Bundy, D.A.P. (1990) *Parasitology* **101,** 417−427.
46. Lambert, D. (1992) *Technometrics* **34,** 1−14.

Figure legend

Figure 3. Observed (closed circles) and fitted (solid lines) age-profiles of the examined population by country. Markers represent averages of observations within 3-yr age groups; lines represent fitted negative exponential functions.

Table 4. Other parameters of the model

Parameter	Definition	Value and units			Source
		Cameroon	Guatemala	Venezuela	
σ_L	Per capita mortality rate of L3 larvae		104 yr^{-1}		(22, 29)
μ_V	Per capita mortality rate of uninfected vectors		52 yr^{-1}		(22, 29)
α_V	Excess vector mortality rate induced per mf	0.60 yr^{-1}	0.43 yr^{-1}	0.60 yr^{-1}	(29)
ϕ	Adult worm mating probability		1		(6, 22)
F	Per capita fecundity rate of female adult worm scaled per mg of skin		0.67 yr^{-1}		(22, 34)
δ_{H_0}	Maximum establishment probability of an L3 larva within a human (as transmission rate tends to zero)		8.54 x 10^{-2}		¶
δ_{H_∞}	Minimum establishment probability of an L3 larva within a human (as transmission rate becomes infinitely large)		2.99 x 10^{-2}		(29)
c_H	Severity of transmission rate-dependent constraints upon larval establishment within humans		5.86 x 10^{-}3 yr		(29)
δ_{V_0}	Probability that a mf becomes an L3 larva within the vector (in the absence of density dependence)	0.0050	0.0005	0.0015	‖
a_H	Probability that an L3 larva is shed during a blood meal		0.5		(20, 27)

¶ In line with the value of 7.12 x 10^{-2} (3.82 x 10^{-2}, 14.91 x 10^{-2}) estimated in (29).
‖ The difference with respect to values previously estimated (29) compensates for the lack of density-dependent larval establishment within the vector in this model and is consistent with the relative competence of the various vector species.

Figure 3

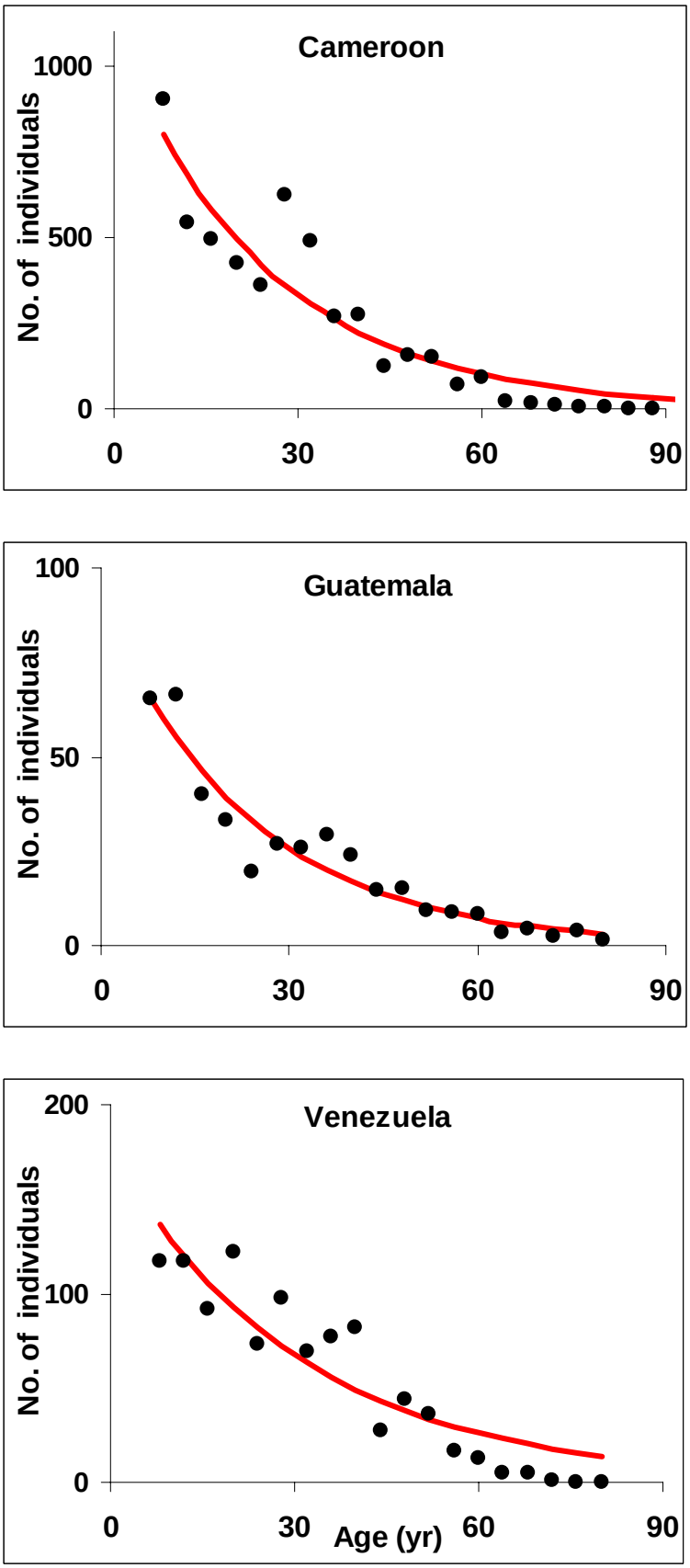
Cameroon
No. of individuals
1000
500
0
0
30
60
90
Guatemala
No. of individuals
100
50
0
0
30
60
90
Venezuela
No. of individuals
200
100
0
0
30
60
90
Age (yr)